This manuscript has been submitted for publication in Paleoceanography-Paleoclimatology. *It has not yet undergone peer review and will probably change somewhat before it is accepted. If accepted, the final version of the manuscript will be available via the "Peer-reviewed Publication DOI" link on the EarthArXiv page. Please feel free to contact the authors with feedback.*

Early Paleocene Paleoceanography and Export Productivity in the Chicxulub Crater

Christopher M. Lowery[1]*, Heather L. Jones[2], Tim Bralower[2], Ligia Perez Cruz[3], Catalina Gebhardt[4], Michael T. Whalen[5], Elise Chenot[6], Jan Smit[7], Marcie Purkey Phillips[1], Konstantin Choumiline[8], Ignacio Arenillas[9], Jose A. Arz[9], Fabien Garcia[10], Myriam Ferrand[10], Johanna Lofi[6], Sean P.S. Gulick[1], Exp. 364 Science Party[11]

[1]Institute for Geophysics, Jackson School of Geosciences, University of Texas at Austin, USA

[2]Department of Geosciences, Pennsylvania State University, University Park, USA

[3]Instituto de Geofísica, Universidad Nacional Autónoma De México, Ciudad de México, México

[4]Alfred Wegener Institute Helmholtz Centre of Polar and Marine Research, Bremerhaven, Germany

[5]Department of Geosciences, University of Alaska Fairbanks, USA

[6]Géosciences Montpellier, Université de Montpellier, France

[7]Faculty of Earth and Life Sciences (FALW), Vrije Universiteit Amsterdam, Netherlands.

[8]Department of Earth Sciences, University of California Riverside, USA

[9]Departamento de Ciencias de la Tierra and Instituto Universitario de Investigación en Ciencias Ambientales de Aragón, Universidad de Zaragoza, E-50009, Spain

[10]Biogéosciences, Université de Bourgogne Franche-Comté, France

[11]See Appendix 1

Corresponding author: Christopher Lowery (cmlowery@utexas.edu)

Key Points (three, 140 characters each)

- Export productivity in the Chicxulub crater is high for the first 300 kyr after the K-Pg boundary

- Water column stratification is variable for the first ~Myr of the Paleocene; changes in stratification associated with nannofossil turnover
- Many other sites show similar changes ~65.7 Ma, suggesting global change in circulation possibly linked to the coeval Dan-C2 hyperthermal

Abstract

The Chicxulub impact caused a crash in export productivity in much of the world's oceans which contributed to the extinction of 75% of marine species. In the immediate aftermath of the extinction, local export productivity was highly variable, with some sites, including the Chicxulub crater, recording elevated export production. The long-term transition back to more stable export productivity regimes has been poorly documented. Here, we present elemental abundances, foraminiferal and calcareous nannoplankton assemblage counts, total organic carbon, and stable carbon isotopes from the Chicxulub crater to reconstruct long-term changes of productivity over the first 3 Myr of the Paleocene. We show that export production was high for the first 300 kyr of the Paleocene and then declined for the next 700 kyr. This decline is broadly associated with increasing water column stratification. A final decrease in export productivity occurred after ~ 1 Myr. We suggest that increasing upper water column stratification reduced the availability of nutrients in the photic zone, which drove an increase in the efficiency of the biological pump. Increased pump efficiency created a positive feedback which drove the further development of oligotrophic conditions; the onset of oligotrophy perturbed the stable disaster nannoplankton assemblage and allowed other taxa to gain a foothold in the ecosystem. The initial decline in export productivity 300 kyr after the boundary is observed across the globe and may have been an important driver of turnover in post-extinction communities. We postulate that these changes are related to the Dan-C2 hyperthermal event.

Plain Language Summary

The end Cretaceous mass extinction was caused by the impact of an asteroid on the modern Yucatán Peninsula, Mexico. The impact ejected aerosols and dust into the air that blocked out the sun, causing a severe decline in photosynthesis and the collapse of marine food webs. However, the change in the amount of food created by photosynthesizing plankton that makes it to the seafloor (export productivity) was not temporally or spatially uniform across the oceans. At some places, including the Chicxulub crater, export productivity was actually high immediately after the impact. We produced an extended ~3 million year record of export productivity in the crater to determine how long it remained high and why it eventually declined. Export production was very high for the first 300,000 years after the impact and remained elevated for the next 700,000 years. It eventually declined due to changes in mixing in the surface ocean which affected how efficiently nutrients were removed from the surface ocean to the deep sea. This decline caused a change in the population of fossilized primary producers from a few species adapted to high nutrient, high productivity conditions to a diverse population better adapted for low nutrient, low productivity conditions.

Keywords: K-Pg, Chicxulub Crater, Paleoproductivity, Foraminifera, Nannoplankton, Paleocene, Dan-C2 Hyperthermal

1. Introduction

At the end of the Cretaceous Period (~66 Ma), the impact of an asteroid on the Yucatán platform in the southern Gulf of Mexico caused the extinction of 75% of species on Earth, including ~90% of pelagic calcifiers such as planktic foraminifera and calcareous nannoplankton (Alvarez et al., 1980; Smit et al., 1980; Hildebrand et al., 1991; Jablonski, 1995; Schulte et al., 2010, Fraass et al., 2015; Knoll and Follows, 2016). Dust and sulfate aerosols ejected from the carbonate and evaporite-rich target rock, as well as soot from possibly global wildfires, blocked the sun, resulting in severe short-term cooling (Vellekoop et al., 2014, 2016; Bardeen et al., 2017 Brugger et al., 2017; Artemieva et al., 2017; Gulick et al., *in press*) and collapse of the food chain due to a sharp decline in photosynthesis (Zachos et al., 1989; D'Hondt et al., 1998; Kring, 2007). These effects were short-lived, however, as most dust, soot, and

aerosols were removed from the atmosphere on the order of years (Brugger et al., 2017), and the oceans quickly became hospitable, even at ground zero in the Chicxulub crater (Lowery et al., 2018).

The recovery of marine primary productivity was a crucial first step in the overall recovery of the ocean ecosystem after this apocalypse. Understanding this process has long been a goal of researchers interested in the recovery of life after major mass extinctions (e.g., Hsü and McKenzie, 1985). Early records of productivity after the Cretaceous-Paleogene (K-Pg) mass extinction derived from carbon isotopes show that the vertical gradient of $\delta^{13}C$, developed by the export of organic carbon from the surface ocean to the seafloor, collapsed in the early Danian for about 1.8 Myr (Hsü and McKenzie, 1985; Zachos et al., 1989; D'Hondt and Zachos, 1998; Coxall et al., 2006; Birch et al., 2016). This was initially interpreted as evidence of complete or nearly complete cessation of surface ocean productivity, an idea which became known as the Strangelove Ocean (Hsü and McKenzie, 1985). Later, D'Hondt et al. (1998) suggested that surface ocean productivity continued but that the disappearance of larger organisms prevented the export of organic matter to the deep sea (known as the Living Ocean hypothesis). The observed changes in the carbon isotope gradient can be explained by a small increase in the percentage (e.g., from 90 to 95%) of the organic matter that is remineralized in the upper ocean (D'Hondt et al., 1998; Alegret et al., 2012).

There is a great deal of data indicating continued organic carbon flux to the deep sea in the early Danian. Benthic foraminifera, which are entirely dependent on the flux of organic matter from above for food, did not suffer extinction at the K-Pg boundary (Culver, 2003; Alegret et al., 2012). Biogenic barium, a paleoproductivity proxy which has been shown to correlate with organic matter flux from overlying surface water, i.e., *export* productivity (e.g., Griffith and Paytan, 2007), indicates that export production did not uniformly decline across the oceans, as some sites actually show an increase in export the period after the Chicxulub impact (Hull and Norris, 2011). Broadly, sites in the Gulf of Mexico/North Atlantic/Tethys region record reduced export production in the early Danian (Alegret et al., 2001; Esmery-Senlet et al., 2015; Vellekoop et al., 2017), whereas sites in the central Pacific record increased

export production during the same time period (Hull and Norris, 2011). This geographic heterogeneity was proposed to be driven by the uneven distribution of toxic metals in the ocean, related to distance from the Chicxulub crater and the angle of the impact, interpreted to be from south to north (Jiang et al., 2010). However, new modelling based on geophysical datasets and results from recent International Ocean Discovery Program/International Continental Drilling Program (IODP/ICDP) joint Expedition 364, which drilled the peak ring of the Chicxulub crater (Morgan et al., 2017), has found that the angle of impact was steeply inclined and that the direction was towards the southern hemisphere (Collins et al., in review; Lowery et al., 2019). Moreover, cores taken just above the impact-generated rocks show evidence of the rapid establishment of a healthy, high-productivity ecosystem in the crater within 30 kyr of the impact (Lowery et al., 2018). This was an order of magnitude quicker than the recovery of export productivity at other Gulf of Mexico/North Atlantic sites, which suggests that differences in marine productivity were not driven by distance from the crater, impact direction, or linked environmental factors. Rather, it appears that this post-impact heterogeneity must be controlled by more seemingly "random" ecological factors like incumbency and competitive exclusion (Hull et al., 2011; Schueth et al., 2015; Lowery et al., 2018).

It is unclear how long high export productivity persisted at ground zero, and how it relates to global patterns of heterogeneous export production in the early Danian. Was this locality oceanographically pre-disposed to high export productivity, or did changing conditions eventually lead to a decline? If so, what conditions shifted to cause lower export production?

The answers to these questions, particularly the cause of the shift from heterogeneous post-impact export productivity regimes to whatever succeeded them, also have important bearing on our understanding of the biological recovery after the Chicxulub impact. Perhaps surprisingly, given the rapid recovery of export productivity and the high diversity of planktic foraminifera, the recovery of calcareous nannofossil diversity was delayed within the Chicxulub crater. Disaster taxa, including cyst-forming dinoflagellates such as *Cervisiella* (a genus previously known as *Thoracosphaera*) and the eutrophic

nannoplankton *Braarudosphaera*, dominated nannofossil assemblages for a million years after the K-Pg boundary (Jones et al., 2019). Ecological experimentation, exemplified by a series of acmes of taxa which rapidly increased then declined in abundance ("boom-bust successions"), began ~ 1 Myr after the impact (Jones et al., 2019), well after similar successions at other sites had subsided (e.g., Bown, 2005; Schueth et al., 2015). Jones et al. (2019) attributed the persistence of disaster species within the Chicxulub crater to high productivity for the first million years of the Paleocene. These disaster taxa were better adapted to high nutrient conditions, and thus likely outcompeted other calcareous phytoplankton until nutrient concentrations began to decline, at which point a more diverse ecosystem was slowly established via boom-bust successions. Export productivity and photic zone nutrient concentrations are thus believed to be fundamental to ecological recovery (Jones et al., 2019). Understanding the timing and driver(s) of changes in export productivity is essential to constrain the fundamental controls on the early recovery of phytoplankton diversity.

There are a number of environmental changes which may have influenced changes in export productivity in the early Danian. Deccan volcanism began in the Maastrichtian and continued until approximately 65.6 Ma (Schoene et al., 2019) to 65.4 Ma (Sprain et al., 2019), or 400 kyr to 600 kyr after the boundary. Environmental effects of Deccan volcanism have been proposed as a mechanism to delay the recovery of life following the K-Pg mass extinction (e.g., Gertsch et al., 2011; Renne et al., 2015; Punekar et al., 2014a,b), although it is often unclear what is meant by "recovery." Lowery and Fraass (2019) found no relationship between the recovery of planktic foraminifer species diversity and the "main phase" of Deccan volcanism (or its subsequent termination) in the earliest Danian. Perhaps Deccan volcanism instead exerted some influence on the recovery of export productivity. Meanwhile, the first Paleogene hyperthermal event occurred a mere 300 kyr after the K-Pg boundary. The Dan-C2 hyperthermal is characterized by two negative carbon isotope excursions coincident with a similar double spike in clay content and Fe content, and decrease in Ca in deep sea cores (Quillévéré et al., 2008; Coccioni et al., 2010). Each excursion lasts ~40 kyr and they are separated by ~100 kyr, which Quillévéré

et al. (2008) interpreted as evidence of an orbital driver. Whatever the root cause, this event clearly had an effect on marine ecosystems, altering assemblages of foraminifera and calcareous nannoplankton and possibly driving eutrophication, shoaling of the lysocline, and deoxygenation (Coccioni et al., 2010). Was the Dan-C2 also responsible for changes in export production?

Here, we examine planktic and benthic foraminifera, calcareous nannoplankton, and major, minor, and trace elements to reconstruct export productivity, water column stratification, terrigenous flux, and phytoplankton population change during the early Paleocene interval (66.0-62.5 Ma) of IODP Site M0077 in the Chicxulub crater (Figure 1). These data are used to determine how long export productivity remained elevated and if its eventual decline is due to changing environmental conditions. We then compare our data from Chicxulub to coeval sites spanning the Paleocene oceans.

2. Material and Methods

In 2016, IODP/ICDP Expedition 364 drilled the peak ring (e.g., Morgan et al., 2016) of the Chicxulub crater (Morgan et al., 2017), coring over 100 m of post-impact Paleogene sediments with nearly 100% recovery. Ten meters of Paleocene pelagic carbonates were recovered at the base of the post-impact section, conformably overlying the top of the impact breccia. The uppermost 40 cm of this interval is cut by four disconformities and spans the middle and late Paleocene; the rest of the section, the focus of this study, spans the earliest to middle Paleocene, and is continuous from 66 to ~62 Ma (Morgan et al., 2017). Planktic foraminiferal and calcareous nannofossil samples were taken from identical depths throughout the core and prepared using standard techniques. To obtain elemental abundance data, cores were scanned on the AVAATECH XRF Core Scanner II at the University of Bremen. Total organic carbon (TOC) and bulk rock stable carbon isotopes were also measured using standard techniques. Please see supplemental information for full discussion of the analytical techniques employed here.

2.1 Age Model

The age model used here (Table 1) is a slightly updated version of that produced by the Expedition 364 Science Party (Gulick et al., 2017). Calcareous nannofossil age determination is based on the CP zonation scheme of Okada and Bukry (1980) following the taxonomic concepts of Perch-Nielsen (1985) and Bown (1998). Planktic foraminifer biostratigraphy is based on the P zones of Berggren and Pearson (2005) as modified by Wade et al. (2011), following the taxonomic concepts of Olsson et al. (1999) and Pearson et al. (2006). Key taxa are illustrated in Figure 2. Calibrated ages assigned to each datum are those reported in Appendix 3 of the Geologic Time Scale 2012 (Gradstein et al., 2012). Because calcareous nannoplankton are poorly preserved at Chicxulub and form diachronous acmes following the K-Pg mass extinction (Jones et al., 2019), zonal markers are either absent or inconsistent with the planktic foraminifer datums. For this reason, we only used the planktic foraminifer biozones to construct the age model (Table 1). Paleomagnetic reversals are not included in the age model because a heterogenous chemical remnant re-magnetization occurred throughout the study interval obscuring the original polarity (Morgan et al., 2017; Gulick et al., *in press*).

3. Results and Discussion

3.1 M0077 Sedimentology and Terrigenous Flux

The Paleocene interval at Site M0077 is primarily pelagic carbonate with varying degrees of dilution by terrigenous material (Figure 3). We reconstruct terrigenous flux using several elemental proxies and magnetic susceptibility (Figure 3). Iron is generally correlated with terrigenous sediments, while calcium is primarily sourced from marine calcifiers. Both Fe and Ca are often used to infer carbonate dissolution in deep sea cores, particularly during the Paleogene, which was characterized by discrete episodes of CO_2 release, warming, and ocean acidification (Bralower et al., 2002; Edgar et al., 2007; Quillévéré et al., 2008; Coccioni et al., 2010). However, we conclude that Fe and Ca variations are driven by changes in dilution rather than dissolution because: (1) Site M0077 is relatively shallow, around 700 m water depth in the Paleocene (Lowery et al., 2018), well above the early Paleocene lysocline; and (2), intervals of elevated Fe/depressed Ca do not correspond to intervals of reduced foraminifer

preservation (Figure 4). Core material at Site M0077 is strongly lithified, and had to be broken down with a mortar and pestle prior to soaking. An unfortunate side effect of this aggressive disaggregation is the fracturing of some fraction of the foraminifera. We did not distinguish foraminifera broken in this way from fragments of foraminifera which may have experienced partial dissolution on the seafloor due to deposition below the lysocline, a common proxy for ocean acidification ("Foram Fractionation Index;" Thunell 1976). In order to establish some quantitative proxy for foraminifer preservation, we instead report the number of individuals in each counted population that could not be identified to the genus level. These "planktic spp." are excluded from population analysis (other than planktic/benthic ratio) but provide a useful approximation of preservation, with more unidentifiable individuals indicating worse preservation. There is a slight positive correlation between Fe and preservation, and a corresponding negative correlation between Ca and preservation (Figure 4). Enhanced preservation in carbonate-poor intervals is likely due to dilution of the pure pelagic carbonate by clay (marls and organic-poor shales generally contain the best-preserved fossils), and thus increases in Fe are interpreted to represent terrigenous flux.

A number of trends in terrigenous flux are evident in the Paleocene interval of Site M0077 (Figure 3). Overall, terrigenous flux was low for the first ~ 1 Myr of the Danian and higher thereafter. Numerous shorter peaks are superimposed on this long-term trend. The base rate of terrigenous flux, particularly in Fe, is elevated in the upper part of the record relative to the low points around 615.6 mbsf (65.4 Ma) and the base of the pelagic limestone. It should be noted that the closest land was > 500 km away in modern central Mexico (Gulick et al., *in press*), and thus terrigenous material transported to Site M0077 was dominated by clay that only slightly diluted the pelagic carbonate. Increases in the terrigenous component, however, are a useful proxy for changes in continental weathering in the Gulf of Mexico basin and likely indicate increased riverine flux, which we postulate drove changes in stratification.

3.2 M0077 Export Productivity

Biogenic barium, primarily preserved in marine sediments as barite ($BaSO_4$), strongly correlates with modern export production (Dymond et al., 1992; Francois et al., 1995; Eagle et al., 2003; Paytan and Griffith, 2007) and is thus a commonly used export productivity indicator (e.g., Payton et al., 1996; Bains et al., 2000; Griffith and Paytan, 2012), including in the early Paleocene (Hull and Norris, 2011). Barite is primarily formed in marine environments during the remineralization of sinking organic matter, but it can also be sourced from terrigenous sediments. Therefore, to isolate the biogenic fraction, barium is normalized to the terrestrially-sourced element titanium (Dymond et al., 1992; Paytan and Griffith, 2007). Different continental drainage basins may have differing Ba/Ti ratios, and thus long-term changes in sediment source area or dust vs. riverine flux may bias the data by indicating apparent changes in export productivity (Payton and Griffith, 2007). However, significant changes in the sediment source to the southern Gulf of Mexico did not occur until the Laramide Orogeny, which began in the late Paleocene and therefore would not have influenced early Paleocene sedimentation (Galloway et al., 2000). Because there is also not a major long-term change in sediment type (pelagic carbonate) over the interval studied here, we consider sedimentary source changes to be an unlikely driver of observed trends in biogenic barium. To test this interpretation, we compare the Ba/Ti export productivity proxy to several other productivity proxies, specifically planktic foraminifer assemblage changes and benthic foraminiferal abundance.

Paleocene planktic foraminifera exhibit several adaptations in their trophic strategies, which allow some groups to thrive in low-nutrient environments. Microperforate and smooth normal perforate planktic foraminifera (*Guembelitria, Globoconusa, Parvularugoglobigerina, Woodringina, Chiloguembelina,* etc.) were grazers, feeding on phytoplankton and any organic detritus that they could catch in their network of rhizopodia. Their food sources did not include most motile zooplankton, which are generally able to free themselves from such unsupported rhizopodal networks (Hemleben et al., 1991). In the early Danian, however, some new genera (*Eoglobigerina* and the Subbotinids) evolved spines, long protrusions of calcite which provide an anchor for the rhizopods and allow them to hold on to motile prey,

enabling these groups to adapt a carnivorous lifestyle and open a new food source: other zooplankton (Hemleben et al., 1991; Olsson et al., 1999). Several million years later, another group of planktic foraminifera acquired photosymbionts, beginning with *Praemurica uncinata* and followed by *Acarinina, Morozovella,* and *Igorina* (Coxall et al., 2006). In the modern ocean, photosymbiont-bearing planktic foraminifera tend to dominate in oligotrophic subtropical gyres. Spinose and symbiont-bearing planktic foraminifera are thus better adapted to food-limited environments, and we expect them to be predominant in oligotrophic waters. On the other hand, non-spinose, non-symbiont bearing planktics, the grazers, are best adapted to eutrophic environments, and should be dominant there.

Benthic foraminifera are also powerful paleoenvironmental indicators. They are primarily sensitive to changes in dissolved oxygen and food supply, with fewer benthics in dysoxic or oligotrophic environments (Jorissen et al., 1995; Gooday, 2003; Van Hinsbergen et al., 2005). Benthic abundance is also often inversely correlated with water depth (e.g., Murray, 1976; Culver, 1988; Van der Zwaan et al., 1990; Leckie and Olson, 2003). The seafloor at Site M0077 was clearly well-oxygenated throughout the study interval, as evidenced by abundant ichnofauna (Morgan et al., 2017). Additionally, the site was located in upper/middle bathyal depths (600-700 m; Gulick et al., 2008; Lowery et al., 2018), and low-amplitude sea level change throughout the early Paleocene (Kominz et al., 2008) should not have affected the %benthics at this depth. With changes in oxygen and sea level thus ruled out, we are confident that food supply to the seafloor (i.e., export production) was the strongest influence on %benthics at Site M0077.

Export productivity was high overall in the early Danian, and broadly declined from 66.0 to ~64.5 Ma (616.5 to ~613.7 mbsf), based on Ba/Ti, %benthics, and planktic trophic groups (Figure 5). Ba/Ti ratios, the highest resolution dataset, show that the interval of highest export productivity terminated sharply around 65.7 Ma (616.2 mbsf). This time interval corresponds to the Dan-C2 hyperthermal (Quillévéré et al., 2008; Coccioni et al., 2010); unfortunately, low sedimentation rates, extensive bioturbation, and diagenetic alteration (expressed as stylolites in the core) mean that the carbon isotope

excursion for this hyperthermal is not preserved in our section. The subsequent period of decline is interrupted by a second peak in export production which occurred around 65.2 Ma (615.1 mbsf), after which export production flattens out. The initial ~1 Myr period of high, generally declining productivity is also evident in the foraminifera. Benthic foraminifera, dependent on the flux of organic matter from above, are abundant overall in the lower Danian, as are non-spinose, non-symbiont bearing planktic foraminifera, which are best suited to eutrophic environments. The rest of the study interval is characterized by low and stable Ba/Ti ratios (with several small short-lived increases), higher abundances of oligotrophic planktic foraminifera, fewer benthic foraminifera, and an increasingly diverse calcareous nannoplankton assemblage.

3.3 Water Column Structure

Planktic foraminiferal paleoecology also provides insight into local hydrography. Planktic foraminifera occupy specific depth habitats in open ocean environments which can be determined via single-species isotopic analysis (e.g., Aze et al., 2011; Birch et al., 2012). The pervasive foraminiferal recrystallization throughout Site M0077 prevents this kind of geochemical analysis, but fortunately we can use the Paleocene compilation of Aze et al. (2011) to assign the species to depth habitats (Table 2). Here, we use the relative proportion of mixed layer, thermocline, and sub thermocline taxa to reconstruct the degree to which the water column was stratified. Dominance of mixed layer taxa indicates the lack of suitable habitat for thermocline/subthermocline species, suggesting weak stratification with the mixed layer habitat extending through much of the photic zone. Higher abundances of thermocline and subthermocline taxa indicate a more stable habitat for these species, which may result from stronger water column stratification. Conversely, a dominance of mixed layer taxa may indicate the presence of an oxygen minimum zone below the mixed layer preventing colonization of those depths except during particular seasons.

Overall, Site M0077 is dominated by mixed layer taxa for the first ~ 200 kyr of the Danian, followed by a shift to more stratified waters from ~ 200-400 kyr (616.3-615.9 mbsf) after the boundary, a return to mixed-layer dominated waters from 400-900 kyr (615.9-614.9 mbsf) after the boundary, and finally a permanent shift toward stable stratified waters after 900 kyr (above 614.9 mbsf).

4. Evolution of surface ocean circulation in the early Chicxulub Crater

Synthesizing this diverse dataset, we interpret a progression from a high productivity, well-mixed water column to one that is oligotrophic and stratified. This progression occurs in several steps (see numbered, shaded bars on Figure 5) as follows:

4.1 High export productivity, well-mixed water column (66.0-65.9 Ma).

The first 100 kyr after the Chicxulub impact (616.5-616.4 mbsf) is characterized by high export production and is dominated by mixed-layer planktic foraminifera, predominantly *Guembelitria*, *Globoconusa*, and *Parvularugoglobigerina*, while the disaster taxon *Cervisiella* dominated the nannoplankton community. Several acmes of planktic foraminifera occurred across the Tethys and North Atlantic after that K-Pg boundary, termed Planktic Foraminiferal Acme Stages (PFAS; Arenillas et al., 2000, 2006, 2016; Alegret et al., 2004). These represent a coeval succession of dominant taxa in open marine sections over a wide geographic area. The presence of these acme stages within the crater (Figure 6) is another indication that the planktic foraminiferal populations are representative of at least regional trends and not local processes unique to the crater. PFAS-1, the predominance of *Guembelitria*, corresponds to this earliest interval of post-impact sedimentary rocks.

4.2 High export productivity, increasing stratification (65.9-65.7 Ma).

During the period from 100-300 kyr after the impact (616.4-616.1 mbsf), high export productivity continued but thermocline and sub-thermocline dwelling foraminifera (*Eoglobigerina* and *Chiloguembelina*) become more common. This transition is coincident with a small increase in

terrigenous flux (see also Figure 3) which we propose led to the increased stratification. PFAS-2, the predominance of *Globoconusa* and *Parvularugoglobigerina*, occurs in this interval (Figure 6).

4.3 Declining export productivity, well stratified water column (65.7-65.6 Ma).

A sharp drop in export productivity occurred 300 kyr after the boundary (616.1 mbsf) during a period of well-developed water column stratification (indicated both by planktic foraminifer assemblages and the first measurable organic carbon). *Braarudosphaera* became predominant in the nannofossil assemblage, although foraminifer-sized calcispheres (tentatively identified as *Cervisiella*) also bloomed at that this time, suggesting that this taxon may have just become larger. This event is not associated with any evidence for increased terrigenous flux. PFAS-3, the predominance of *Woodringina* and the sub-thermocline-dwelling *Chiloguembelina*, also begins in this interval. This correlation suggests that the changes in stratification observed at Site M0077 are part of larger trends that extend at least across the North Atlantic. The observed stratification may have been driven primarily by the warming that occurred at this time, associated with the Dan-C2 hyperthermal, which is not recorded in our carbon isotope data but occurred at 65.7 Ma (Quillévéré et al., 2008). The lack of the diagnostic isotope excursion for this event here is likely due to a combination of low sedimentation rate and pervasive bioturbation combined with diagenetic alteration of the carbonate; there is no stratigraphic evidence for a hiatus at this level, and no change in sedimentation rate to indicate the absence of ~ 200 kyr worth of sediment.

A clear change in export productivity and/or upper water column stratification occurs 300 kyr after the K-Pg boundary at many sites around the globe. In the western Gulf of Mexico, benthic foraminiferal assemblages indicate a return to pre-extinction levels of export production ~300 kyr post impact (Alegret et al., 2001; Alegret and Thomas, 2005), presumably also as a result of the observed regional changes in stratification. Benthic foraminifer assemblages also recover ~300 kyr after the K-Pg boundary on the eastern side of the Atlantic Ocean in Spain (Alegret and Thomas, 2005). PFAS-3 begins around this level, and is characterized in part by a proliferation of *Chiloguembelina* (Arenillas et al., 2000), a sub-thermocline dweller (D'Hondt and Zachos, 1993) also suggesting increased stratification. At

the Gubbio section in Italy, the Dan-C2 hyperthermal is also associated with increased stratification as well as an increase in benthic foraminifer abundance, suggesting higher export productivity or a more efficient biological pump (Coccioni et al., 2010). At Walvis Ridge in the South Atlantic, Foraminifer isotope data also indicate an increase in thermal stratification (Birch et al., 2016). At Maud Rise in the Southern Ocean, low Ba/Ti and Ba/Fe ratios begin to recover ~300 kyr after the K-Pg boundary (Hull and Norris, 2011). At Shatsky Rise in the equatorial Pacific, high post-extinction export productivity spikes and then declines ~300 kyr post impact (Hull and Norris, 2011). These sites are broadly distributed geographically, and represent a range of depositional environments. Although there are other sites at which no change is observed at this point in time (e.g., Vigo Seamount, São Paulo Plateau, and Wombat Plateau; Hull and Norris, 2011), we note that the lack of a globally consistent shift in productivity may be considered analogous to the productivity response to the Paleocene-Eocene Thermal Maximum (PETM), which was dominated by local signals (e.g., Gibbs et al., 2006).

The widespread, global changes in export production 300 kyr after the K-Pg mass extinction occurred at least 100 kyr before the final cessation of Deccan volcanism (Schoene et al., 2019; Sprain et al., 2019), but it is coeval with the Dan-C2 hyperthermal, suggesting a causal link with this hyperthermal and a lack of evidence for any purported cooling effect from the Deccan volcanism (e.g., Fendley et al., 2019). Unfortunately, the Dan-C2 event has seen relatively little study, and its global effects are poorly understood (e.g., Quillévéré et al., 2008 and Coccioni et al., 2010). Although not as well studied as the Eocene hyperthermals, the Dan-C2 event occurs at a critical moment in Earth's history, as the early K-Pg recovery interval came to an end and new Paleocene organisms became established; we suggest that the Dan-C2 hyperthermal event requires additional focused study.

4.4 Moderate export productivity, poorly stratified water column (65.6-65.2 Ma).

400 kyr after the impact (615.9 mbsf), water column stratification weakened and mixed layer taxa again dominated the assemblage. Benthic foraminifera reached their peak abundance, indicating a well-oxygenated seafloor with an adequate food supply. Foraminifer-sized calcispheres peaked and then

declined as *Cervisiella* again dominated the nannofossil assemblage. Microperforate planktic foraminifera, best adapted to eutrophic conditions, still dominated the foraminiferal population, as did eutrophic nannoplankton taxa (i.e., *Cerviseilla* and *Braarudosphaera*). Taken together, the productivity proxies suggest that surface waters were still eutrophic but that export productivity was declining.

4.5 Stratification redevelops and productivity declines (65.2-64.3 Ma)

Over the next ~ million years (615.2-613.2 mbsf) stratification strengthened, indicated by both planktic foraminifera and TOC, while export productivity slowly declined. Total organic carbon is essentially zero for the first million years of the Danian and is higher, although still low, from 65.0-62.5 Ma (Figure 5). TOC enrichment is controlled by both productivity and preservation (e.g., Pederson and Calvert, 1990), so an increase in TOC concurrent with a reduction in export productivity suggests an increase in the preservation potential of organic matter. The most likely mechanism for this increase is reduced ventilation of the seafloor, indicating enhanced stratification at the study area after 65.0 Ma. Increased TOC and decreased export productivity were concurrent with increasing terrigenous flux (Figure 5). Stratification appears to have been linked to increased terrigenous flux, indicated by comparatively elevated Fe, Ti/Al, and magnetic susceptibility through this interval (Figure 3).

Declining export productivity was associated with the decline of nannoplankton disaster taxa and the onset of successive acmes of new taxa ("boom-bust successions," Jones et al., 2019) and an increase in spinose foraminifera, which have a wider diet than non-spinose, non-symbiont-bearing planktics and thus were (and still are) better suited for lower nutrient waters. Jones et al. (2019) suggested that declining productivity was due to the local recovery of the biological pump; our data indicate that this increased pump efficiency was tied to an increase in stratification. Stratification limits the upwelling of deeper, more nutrient rich waters. Nutrient poor waters are, perhaps counter-intuitively, characterized by a more efficient biological pump than eutrophic waters, as a higher proportion of nutrients are exported out of the photic zone (e.g., Hilting et al., 2008). At Site M0077, this change in photic zone nutrient concentrations

disturbed the stable eutrophic disaster nannoplankton assemblage and began a succession of acmes of taxa better adapted to lower nutrient conditions (Figure 6; Jones et al., 2019).

4.6 Stable, Stratified Water Column (64.3-63.5 Ma)

The rest of the lower Paleocene record at Site M0077 (613.2-611.6 mbsf), below a series of stacked unconformities spanning the uppermost Danian to the PETM, documents a stable, stratified, oligotrophic, open-ocean environment. Following the *Praeprinsius* nannoplankton acme, which terminates around 63.4 Ma (Jones et al., 2019), the post-extinction ecosystem was finally stabilized. The lead-up to the Latest Danian Event (LDE – just above the study interval) was also characterized by a well-stratified upper water column at Shatsky Rise in the Pacific Ocean (Jehle et al., 2015). Our results show that in the Gulf of Mexico, at least, increased stratification predates the LDE by several million years.

4.7 Controls on Stratification

The Chicxulub basin was open to the northeast (Gulick et al., 2008) and thus well connected to the rest of the Gulf of Mexico through the entire depth of the crater. The observed changes in stratification (Figure 3) are not, then, the result of restriction in a silled basin. The first major change in stratification, about 65.8 Ma (~616.3 mbsf), is coincident with a small rise in terrigenous flux, likely associated with increased freshwater input into the Gulf of Mexico basin. The elevated terrigenous input declines but the stratification persists during the period of the Dan-C2 hyperthermal event (Quillévéré et al., 2008); the hyperthermal event and local stratification both end around 65.5 Ma (~615.7 mbsf). The re-establishment of a large sub-thermocline population coincides with a second, larger, longer pulse of enhanced weathering that occurred between 65.0 and 65.3 Ma (~615.2-615.0 mbsf), toward the end of the decline in export productivity. The interval of a well-stratified water column after 65.0 Ma (~615.0 mbsf) corresponds to higher background rates of terrigenous flux, and we conclude that changing rates of freshwater input into the

4.8 Global Context

The earliest Danian oceanic environment is often referred to as "unstable" (e.g., Hull et al., 2011). Our data suggest at least one component of this instability is a fluctuating degree of water column stratification, which in turn appears related to changes in export productivity and pelagic ecosystem structure. Overall, stratification appears anti-correlated with export productivity. We conclude that the degree of stratification is a likely driver for the observed trends in export productivity. A well-mixed water column could sustain enhanced primary productivity by delivering nutrients to the photic zone, while a stratified water column limits such mixing. Increased biological pump efficiency at lower nutrient levels (e.g., Hilting et al., 2008) facilitated increased oligotrophy once stratification caused an initial decline in photic zone nutrient content. An increase in stratification, driven by an increase in freshwater flux into the Gulf of Mexico, could thus lead to the observed shift from eutrophic to oligotrophic waters.

Strengthening stratification corresponds to the decline in the dominance of *Cervisiella* ~ 200 kyr after the boundary and immediately precedes the beginning of boom-bust successions of calcareous nannoplankton (Jones et al., 2019) ~1 Myr after the K-Pg boundary. We propose that stratification-moderated changes in nutrient content were the ultimate control on the anomalously long delay in the recovery of species diversity in calcareous nannoplankton at ground zero (Jones et al., 2019). Global changes in stratification around 300 kyr after the boundary, possibly related to the Dan-C2 hyperthermal, provide an explanation for observed changes in export production that occurred at that time.

4. Conclusions

High export productivity in the Chicxulub crater decreased sharply ~300 kyr after the K-Pg boundary at 66 Ma, slowly declined for another 700 kyr, and then remained low through the next ~ 1 Myr, through ~63 Ma. The record of increased stratification and decreased export production at Site M0077, concurrent with an increase in biological pump efficiency, are the likely cause of the observed decline of the post-impact nannoplankton disaster assemblages and the diversification characterized by successive blooms of Paleocene taxa (Jones et al., 2019). A shift in export production around 300 kyr into the Danian is a feature of many records across the oceans and indicates that the trends in export

productivity at Site M0077 are not unique to the crater. Instead, declining productivity appears to be initiated by increased stratification in the Gulf of Mexico, caused both by warming during the Dan-C2 hyperthermal and by a general increase of freshwater input into the Gulf, and sustained by increases in biological pump efficiency. The sharp decline in export production during the Dan-C2 coincides with changes in productivity and stratification at many sites across the world, and we believe that this indicates that a global increase in stratification disturbed recovery ecosystems, spurred a recovery of the biological pump, and drove a turnover in the plankton.

Data Availability Statement

Planktic foraminifer data and XRF core scan data will be uploaded to the NOAA National Climate Data Center before publication. Calcareous nannoplankton data are from Jones et al. (2019) and are archived as GSA Data Repository Item 2019271.

Acknowledgements

The authors acknowledge NSF OCE 1737351. We are grateful to Pincelli Hull for her helpful discussions on our data and hers, and to the staff of the Bremen Core Repository for their invaluable help sampling and scanning the core. We also thank Tessa Cayton for her assistance preparing foraminifer samples. I.A. and J.A.A. acknowledge the use of the Servicio General de Apoyo a la Investigación-SAI, Universidad de Zaragoza. The European Consortium for Ocean Research Drilling (ECORD) implemented Expedition 364 with funding from the International Ocean Discovery Program (IODP) and the International Continental scientific Drilling Project (ICDP). Data and samples can be requested from IODP. U.S. participants in Exp. 364 were supported by the U.S. Science Support Program. J.V.M. was funded by NERC, Grant: NE/P005217/1. I.A. and J.A.A. were supported by MINECO/FEDER-UE (project number CGL2015-64422-P) and MCIU/AEI/FEDER, UE (project number PGC2018-093890-B-I00). This is UTIG Contribution #XXXX.

Appendix 1

Expedition 364 Science Party: Elise Chenot, Gail Christeson, Philippe Claeys, Charles Cockell, Marco J. L. Coolen, Ludovic Ferrière, Catalina Gebhardt, Kazuhisa Goto, Sophie Green, Sean Gulick, Heather Jones, David A. Kring, Johanna Lofi, Christopher M. Lowery, Claire Mellett, Joanna Morgan, Rubén Ocampo-Torres, Ligia Perez-Cruz, Annemarie Pickersgill, Michael Poelchau, Auriol Rae, Cornelia Rasmussen, Mario Rebolledo-Vieyra, Ulrich Riller, Honami Sato, Jan Smit, Sonia Tikoo, Naotaka Tomioka, Jaime Urrutia-Fucugauchi, Michael Whalen, Axel Wittmann, Long Xiao, Kosei Yamaguchi, William Zylberman

Table 1. Biostratigraphic datums for the Paleocene interval of Hole M0077A. Nannofossil datums marked with asterisks are not used in the age model. Datum ages after Gradstein et al. (2012).

Taxon	Zone	Sample Above	Sample Below	**Avg. Depth**	**Datum Age**
Discoaster multiradiatus	Base of CP8	607.26	607.37	**607.315**	**57.21**
Morozovella acuta	Base of P4b	607.52	607.76	**607.65**	**57.79**
*Heliolithus kleinpellii**	Base of CP5	607.52	607.76	**607.65**	**59.94**
Igorina pusilla	Base of P3a	609.28	609.3	**609.29**	**62.6**
Praemurica uncinata	Base of P2	610.6	610.65	**610.63**	**63**
Globanomalina compressa	Base of P1c	612.36	612.41	**612.385**	**63.9**
*Chiasmolithus danicus**	Base of CP2	612.5	612.75	**612.625**	**64.81**
Subbotina triloculinoides	Base of P1b	615.21	615.26	**615.235**	**65.25**
Parvularugoglobigerina eugubina	Base of P1a	616.15	616.2	**616.175**	**65.72**
Parvularugoglobigerina eugubina	Base Pα	616.56	616.56	**616.56**	**66**

498 **Table 2.** Planktic foraminifer depth habitat assignments based on the ecogroups of Aze et al., 2011. All assignments are from that paper unless

499 otherwise noted. No taxa assigned to Groups 5 and 6 appear in our dataset.

Aze et al. 2011 ecogroups	Group	Explanation	Members
Group 1	Open ocean mixed-layer tropical/subtropical, with symbionts	Very heavy $\delta^{13}C$ and relatively light $\delta^{18}O$	*Morozovella, Igorina, Acarinina, Praemurica inconstans*~,
Group 2	Open Ocean mixed-layer tropical/subtropical, without symbionts	$\delta^{13}C$ lighter than species with symbionts; also relatively light $\delta^{18}O$	*Guembelitria**, *Parvularugoglobigerina**, *Woodringina**, *Globoconusa daubjergensis**†, *Rectuvigerina cretacea**, *Praemurica taurica*, *Preamurica pseudoinconstans*, *Subbotina triangularis*, *Praemurica uncinata*
Group 3	Open Ocean thermocline	Light $\delta^{13}C$ and relatively heavy $\delta^{18}O$	*Globanomalina, Eoglobogerina Parasubbotina varianta, Subbotina trivialis, Subbotina triloculinoides*
Group 4	Open Ocean sub-thermocline	Very light $\delta^{13}C$ and very heavy $\delta^{18}O$	*Chiloguembelina midwayensis**, *Chiloguembelina morsei*^, *P. pseudobulloides*
Group 5	High Latitude	Species only found in high latitude sites	N/A
Group 6	Upwelling/high productivity	Species only found in sites of high productivity or upwelling	N/A

*Olsson et al., 1999 and references therein

†Olsson (1999): "Although its abundance in near-shore sequences indicates a near-surface planktic habitat (Troelsen, 1957; Keller, 1989; Liu and Olsson, 1992), its oxygen isotopic signature and open-marine abundance patterns suggest a preference for relatively cool water masses (Premoli Silva and Boersma, 1989; D'Hondt and Keller, 1991; Liu and Olsson, 1992; D'Hondt and Zachos, 1993)."

~Norris (1996) and Birch et al. (2012) describe *P. inconstans* as first symbiont-bearing planktic.

^no isotope data are available for any other Paleocene Chiloguembelinids, so we place *Ch. morsei* in this group based on the data from its cousin *Ch. midwayensis.*

500

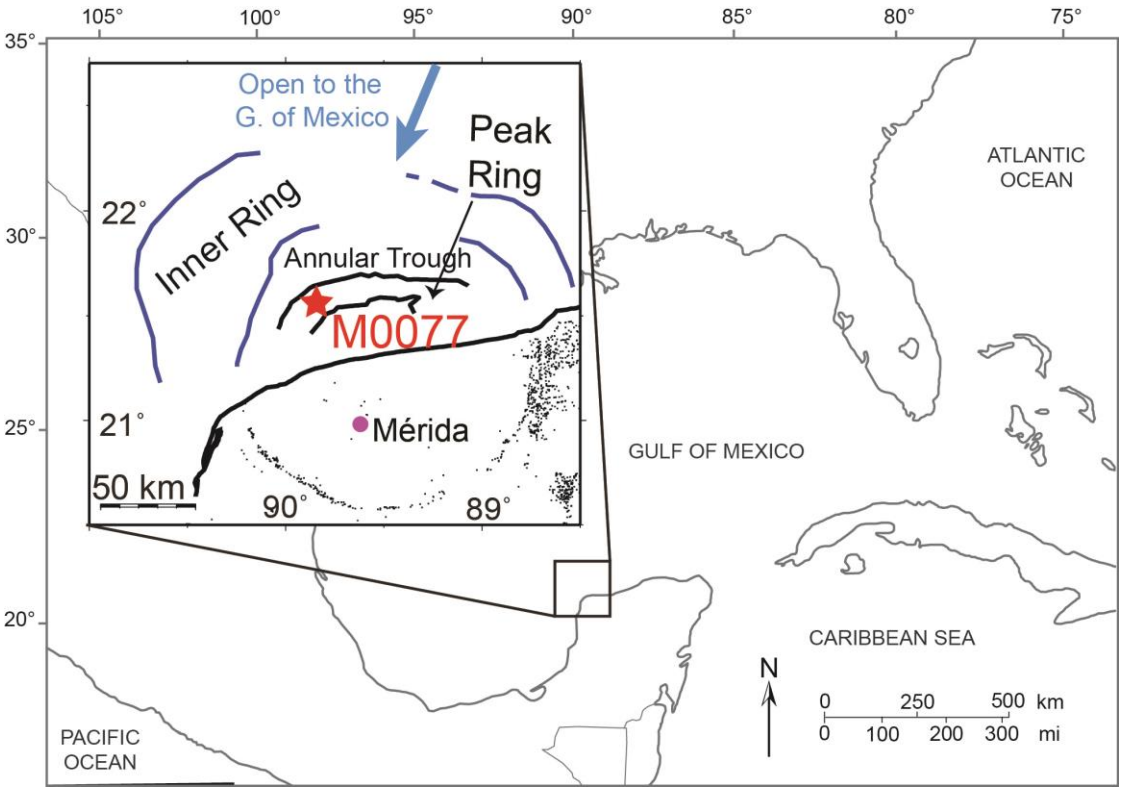

501

502 **Figure 1.** Location map showing the position of IODP Site M0077 within the Chicxulub crater.

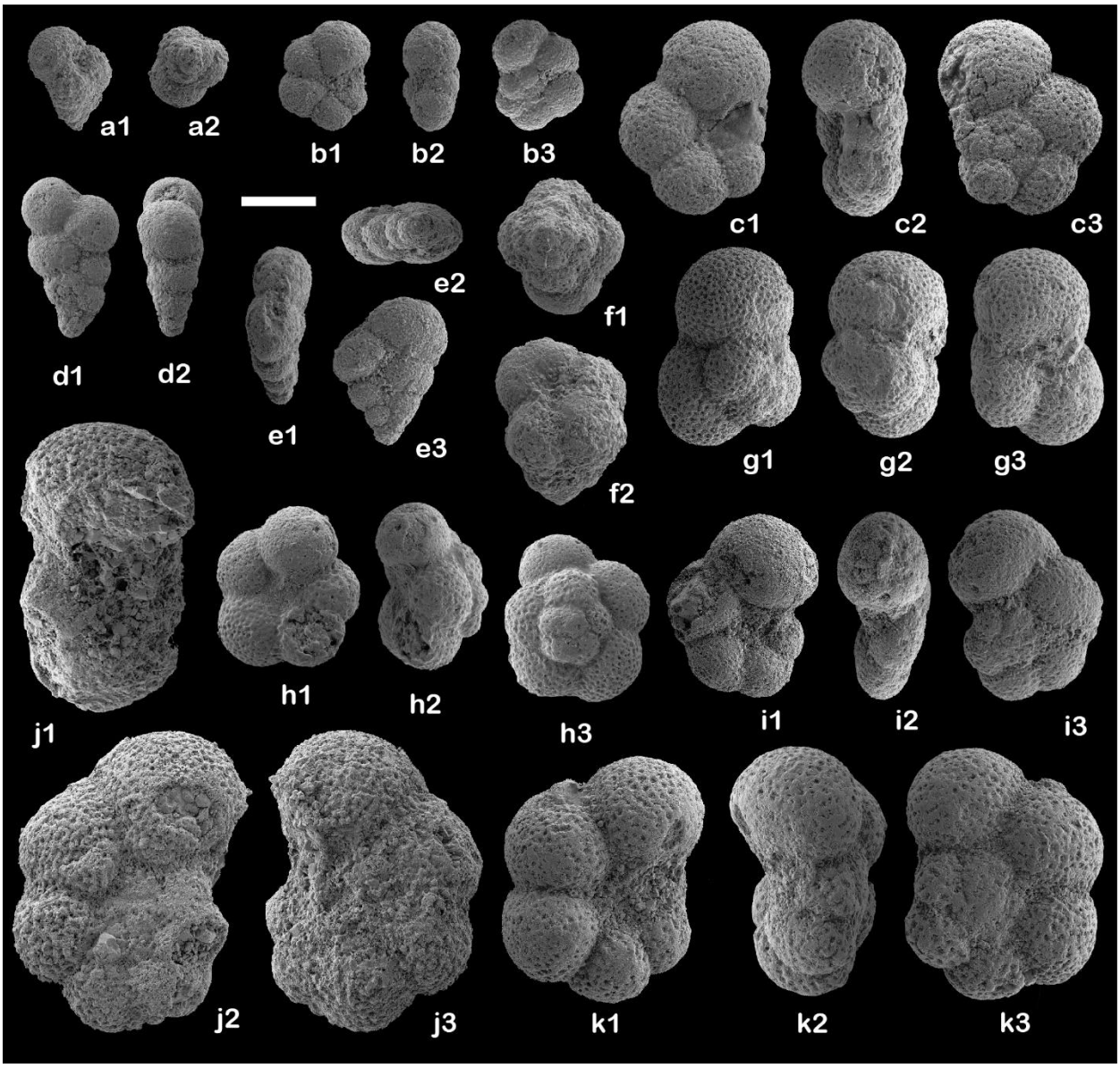

Figure 2. SEM images of planktic foraminiferal index-species and other relevant species (scale bar = 100 microns). (a) *Guembelitria cretacea* (364-M0077A-39R-2 85-86 cm); (b) *Parvularugoglobigerina eugubina* (364-M077A-40R-1 17-18 cm); (c) *Parasubbotina pseudobulloides* (364-M0077A-39R-1 128-129 cm); (d) *Chiloguembelina morsei* (364-M0077A-39R-2 98-99 cm); (e) *Chiloguembelina midwayensis* (364-M0077A-39R-3 41-42 cm); (f) *Globoconusa daubjergensis* (364-M0077A-37R-2 116-117 cm); (g) *Subbotina triloculinoides* (364-M0077A-38R-2 60-61 cm); (h) *Eoglobigerina edita* (364-M077A-38R-2 60-61 cm); (i) *Globanomalina compressa* (364-M0077A-37R-1 116-117 cm);

(j) *Praemurica uncinata* (364-M077A-37R-1 96-97 cm); (k) *Praemurica inconstans* (364-M0077A-37R-2 37-38 cm).

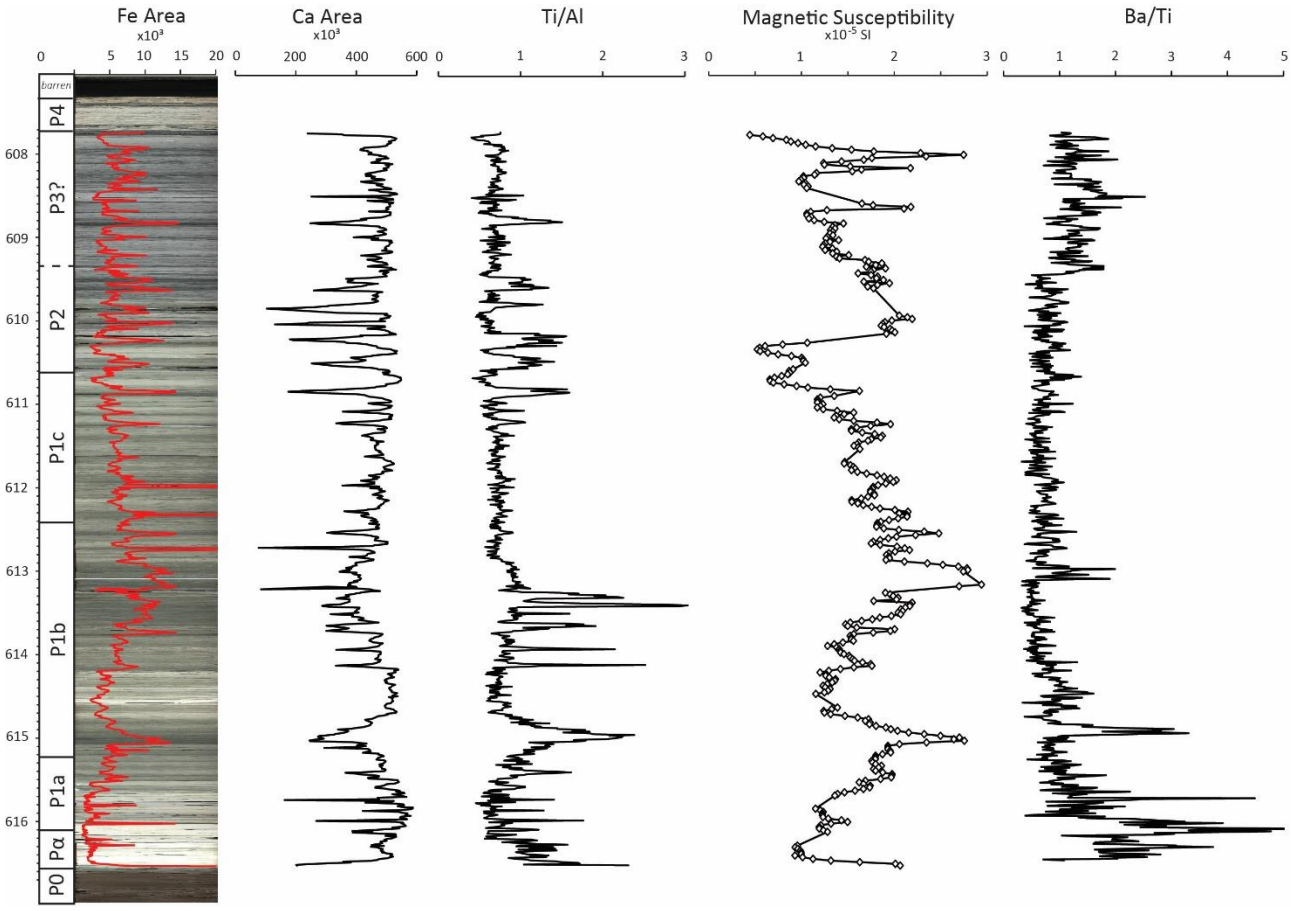

Figure 3. Sedimentological proxies vs. depth. Core linescan composite of the Paleocene interval at Site M0077 is overlaid by XRF Fe counts. Increased Fe, decreased Ca, increased Ti/Al, and higher magnetic susceptibility are all proxies for higher terrigenous flux. Increased Ba/Ti indicated higher local export productivity.

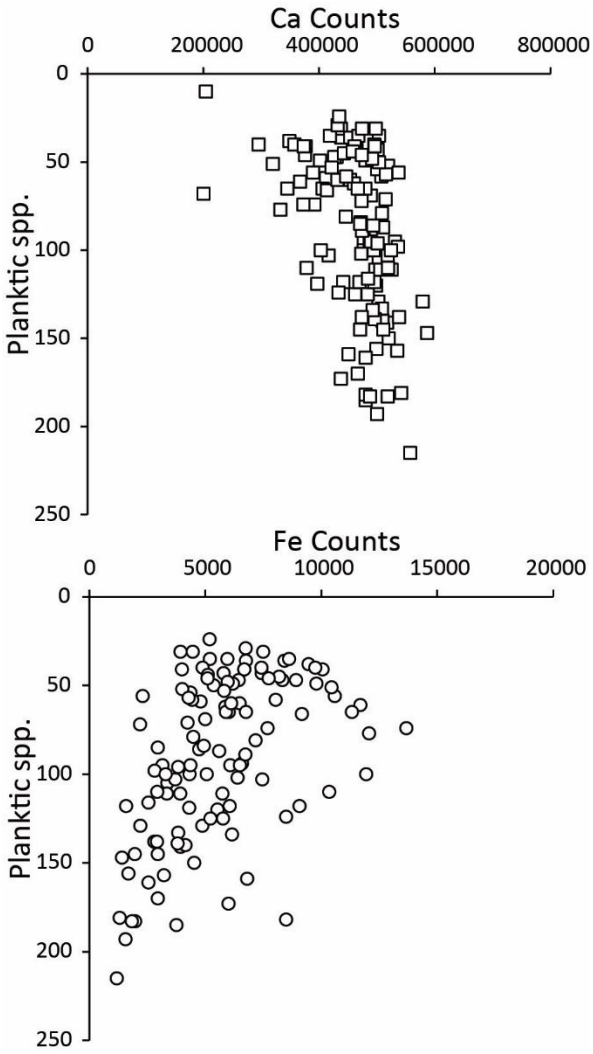

Figure 4. Preservation vs Calcium and Iron XRF counts. Better preservation is toward zero on the y-axis (i.e., fewer unidentifiable foraminifera). Two outliers >80,000 from pyrite-rich samples at the base of the section were removed from the Fe plot. Ca shows a weak negative correlation with good preservation while Fe shows a weak positive correlation with good preservation. This pattern is the opposite of what would be expected if these trends were caused by dissolution.

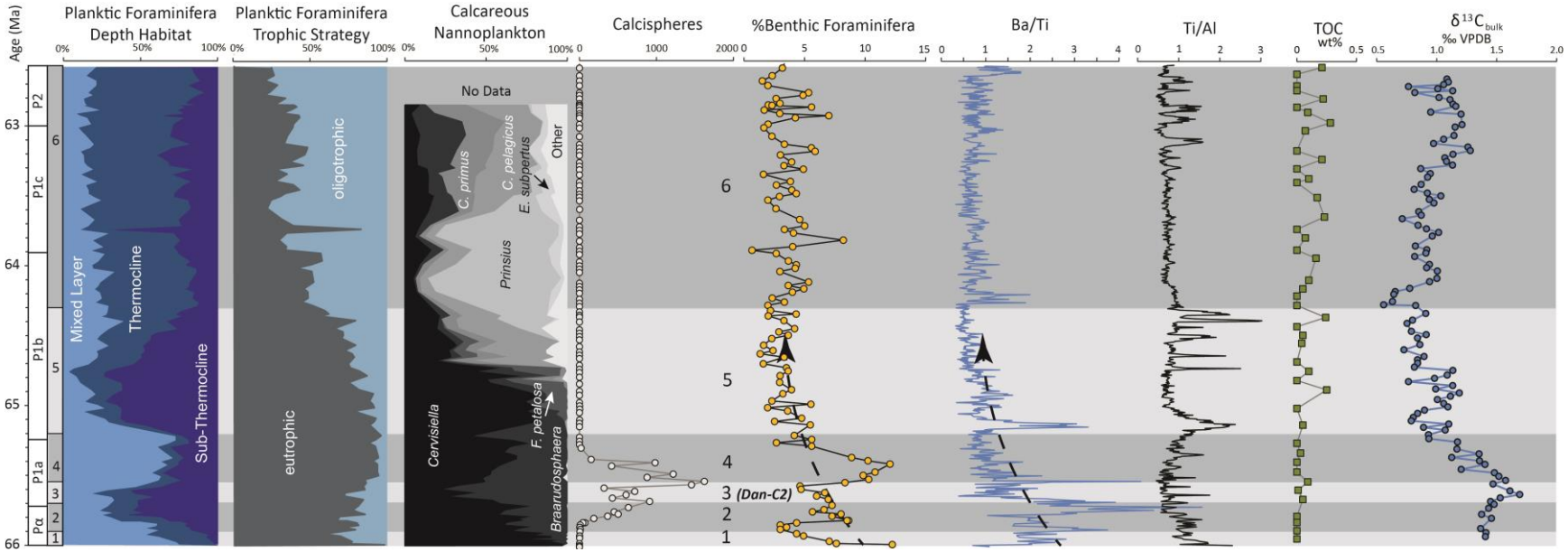

524

525 **Figure 5.** Paleoceanography proxies plotted by age. Planktic foraminifer by depth habitat record the stratification of the upper water column; see
526 Table 2 for species assigned to mixed layer, thermocline, and subthermocline planktic foraminifer groups. Planktic foraminifera by trophic strategy
527 record changes in paleoproductivity, Calcareous nannoplankton diversity shows the relative abundance of all (non-reworked) species of calcareous
528 nannoplankton present. Calcispheres shows the abundance of calcispheres >45 μm. %Benthics is the percentage of benthic foraminifera relative to
529 all foraminifera, and probably responds primarily to nutrient flux to the seafloor. Ba/Ti records paleoproductivity, with high ratios indicating high
530 productivity. Ti/Al records terrigenous flux (see Fig. 4) and TOC (total organic carbon) corresponds to changes in preservation potential at the
531 seafloor; here, preservation increase is probably due to water column stratification.

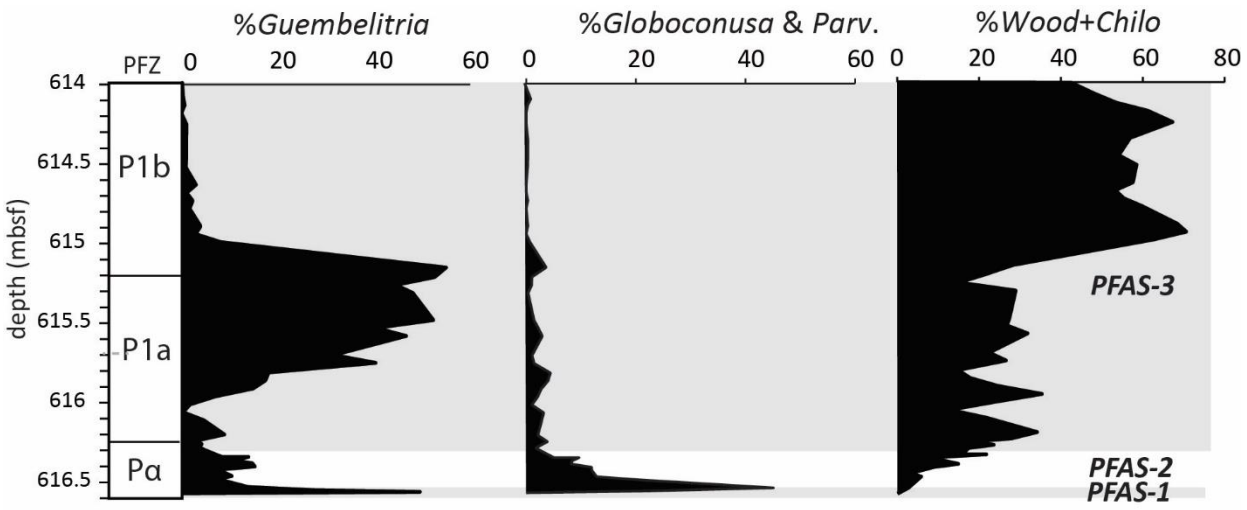

Figure 6. Quantitative stratigraphic distribution of early Danian planktic foraminiferal groups at Site M0077 and Planktic Foraminiferal Acme Stages (PFAS) 1-3: PFAS-1 is the predominance of *Guembelitria*, PFAS-2 is the predominance of *Parvularugoglobigerina* and *Globoconusa* (or *Palaeoglobigerina* according to Arenillas and Arz, 2017), and PFAS-3 is the predominance of *Woodringina* and *Chiloguembelina*. A second acme of *Guembelitria* (or *Chiloguembelitria* according to Arenillas and Arz, 2017) occurs within this stage across the Tethys, as is also evident at Site M0077.

REFERENCES

Alegret, L., Molina, E., & Thomas, E. (2001). Benthic foraminifera at the Cretaceous-Tertiary boundary around the Gulf of Mexico. *Geology*, 29, 891-894.

Alegret, L., & Thomas, E. (2005). Cretaceous/Paleogene boundary bathyal paleo-environments in the central North Pacific (DSDP Site 465), the Northwestern Atlantic (ODP Site 1049), the Gulf of Mexico and the Tethys: The benthic foraminiferal record. *Palaeogeography, Palaeoclimatology, Palaeoecology*, 224, 53-82.

Alegret, L., Arenillas, I., Arz, J. A., & Molina, E. (2004). Foraminiferal event-stratigraphy across the Cretaceous/Paleogene boundary. *Neues Jahrbuch für Geologie und Paläontologie - Abhandlungen*, 234, 25-50.

Alegret, L., E. Thomas, & K.C. Lohmann (2012), End-Cretaceous marine mass extinction not caused by productivity collapse, Proceedings of the National Academy of Sciences, 109(3), 728-732.

Alvarez, L.W., Alvarez, W., Asaro, F., & Michel, H.V., 1980. Extraterrestrial cause of the Cretaceous–Tertiary extinction. Science 208, 1095–1108.

Arenillas, I., Arz, J. A., Molina, E., & Dupuis, C. (2000). An independent test of planktic foraminiferal turnover across the Cretaceous/Paleogene (K/P) boundary at El Kef, Tunisia; catastrophic mass extinction and possible survivorship. *Micropaleontology*, 46, 31-49.

Arenillas, I., Arz, J.A., Grajales-Nishimura, J.M., Murillo-Muñetón, G., Alvarez, W., Camargo-Zanoguera, A., Molina, E., Rosales-Domínguez, C. (2006). Chicxulub impact event is Cretaceous/Paleogene boundary in age: new micropaleontological evidence. *Earth and Planetary Science Letters*, 249, 241-257.

Arenillas, I., Arz, J.A., Grajales-Nishimura, J.M., Rojas-Consuegra, R. (2016). The Chicxulub impact is synchronous with the planktonic foraminifera mass extinction at the Cretaceous/Paleogene boundary: new evidence from the Moncada section, Cuba. *Geologica Acta*, 14(1), 35-51.

Arenillas, I., Arz, J.A. (2017). Benthic origin and earliest evolution of the first planktonic foraminifera after the Cretaceous/Paleogene boundary mass extinction. *Historical Biology*, 29, 17-24.

Artemieva N. et al., 2017, Quantifying the Release of Climate-Active Gases by Large Meteorite Impacts With a Case Study of Chicxulub, *Geophysical Research Letters*, ISSN: 0094-8276

Aze, T., Ezard. T.H.G., Purvis, A., Coxall, H.K., Stewart, D.R.M., Wade, B.S., & Pearson, P.N. (2011), A phylogeny of Cenozoic macroperforate planktonic foraminifera from fossil data, Biological Reviews, 86, 900-927.

Bains, S., Norris, R.D., Corfield, R.M., & Faul, K.L. (2000). Termination of global warmth at the Palaeocene/Eocene boundary through productivity feedback. *Nature*, 407, 171.

Bardeen, C. G., Garcia, R. R., Toon, O. B., & Conley, A. J. (2017). On transient climate change at the Cretaceous− Paleogene boundary due to atmospheric soot injections. *Proceedings of the National Academy of Sciences*, *114*(36), E7415-E7424.

Berggren, W. A., & Pearson, P. N. (2005). A revised tropical to subtropical Paleogene planktonic foraminiferal zonation. *The Journal of Foraminiferal Research*, 35, 279-298.

Birch, H. S., Coxall, H. K., & Pearson, P. N. (2012). Evolutionary ecology of Early Paleocene planktonic foraminifera: size, depth habitat and symbiosis. *Paleobiology*, *38*(3), 374-390.

Birch, H.S., Coxall, H.K., Pearson, P.N., Kroon, D., & Schmidt, D.N. (2016). Partial collapse of the marine carbon pump after the Cretaceous-Paleogene boundary. *Geology*, 44, 287-290.

Boersma, A., & Silva, I.P. (1989). Atlantic Paleogene biserial heterohelicid foraminifera and oxygen minima. *Paleoceanography*, 4, 271-286.

591 Bown, P. (1998). *Calcareous nannofossil biostratigraphy* (pp. 1-315). Chapman and Hall; Kluwer
592 Academic.

593 Bralower, T.J., Silva, I.P. & Malone, M.J., 2002. New evidence for abrupt climate change in the Cretaceous
594 and Paleogene: An Ocean Drilling Program expedition to Shatsky Rise, northwest Pacific. *GSA*
595 *TODAY, 12*, pp.4-10.

596 Brugger, J., Feulner, G., & Petri, S. (2017). Baby, it's cold outside: Climate model simulations of the
597 effects of the asteroid impact at the end of the Cretaceous. *Geophysical Research Letters*, 44,
598 419-427.

599 Coccioni, R., Frontalini, F., Bancalà, G., Fornaciari, E., Jovane, L., & Sprovieri, M. (2010). The Dan-C2
600 hyperthermal event at Gubbio (Italy): Global implications, environmental effects, and
601 cause(s). *Earth and Planetary Science Letters*, 297, 298-305.

602 Collins, G.S., Patel, N., Rae, A.S., Davies, T.M., Morgan, J.V. Gulick, S.P.S. and Expedition 364
603 Scientists (2017). Numerical simulations of Chicxulub crater formation by oblique impact. *Lunar*
604 *and Planetary Science Conference XLVII*, abstract #1832.

605 Coxall, H.K., S. D'Hondt, & J.C. Zachos (2006), Pelagic evolution and environmental recovery after the
606 Cretaceous-Paleogene mass extinction, Geology, 34(4), 297-300.

607 Culver, S.J. (1988), New foraminiferal depth zonation of the northwestern Gulf of Mexico, *Palaios*, 3,
608 69–85.

609 Culver, S. J. (2003). Benthic foraminifera across the Cretaceous–Tertiary (K–T) boundary: a
610 review. *Marine Micropaleontology*, *47*(3-4), 177-226.

611 D'Hondt, S., & Keller, G. (1991). Some patterns of planktic foraminiferal assemblage turnover at the
612 Cretaceous-Tertiary boundary. *Marine Micropaleontology*, 17, 77-118.

613 D'Hondt, S., & Zachos, J.C. (1993). On stable isotopic variation and earliest Paleocene planktonic
614 foraminifera. *Paleoceanography*, 8, 527-547.

615 D'Hondt, S., King, J., & Gibson, C. (1996). Oscillatory marine response to the Cretaceous-Tertiary
616 impact. *Geology*, 24, 611-614.

617 D'Hondt, S., Donaghay, P., Zachos, J.C., Luttenberg, D., & Lindinger, M. (1998). Organic carbon fluxes
618 and ecological recovery from the Cretaceous-Tertiary mass extinction. *Science*, 282, 276-279.

619 D'Hondt, S., & Zachos, J.C. (1998). Cretaceous foraminifera and the evolutionary history of planktic
620 photosymbiosis. *Paleobiology*, 24, 512-523.

621 Dymond, J., Suess, E., & Lyle, M. (1992). Barium in deep-sea sediment: A geochemical proxy for
622 paleoproductivity, *Paleoceanography*, 7, 163-181. doi:10.1029/92PA00181

623 Eagle, M., Paytan, A., Arrigo, K.R., van Dijken, G., & Murray, R.W. (2003). A comparison between excess
624 barium and barite as indicators of carbon export, *Paleoceanography*, 18, 1021.
625 doi:10.1029/2002PA000793

626 Edgar, K.M., Wilson, P.A., Sexton, P.F., & Suganuma, Y., (2007) No extreme glaciation during the main
627 Eocene calcite compensation depth shift, *Nature*, 448, 908-911.

628 Esmeray-Senlet, S., Wright, J.D., Olsson, R.K., Miller, K.G., Browning, J.V., & Quan, T.M. (2015).
629 Evidence for reduced export productivity following the Cretaceous/Paleogene mass extinction,
630 Paleoceanography, 30, doi:10.1002/2014PA002724.

631 Fraass, A.J., Kelly, D.C., & Peters, S.E. (2015), Macroevolutionary history of the planktic
632 foraminifera *Annual Reviews of Earth and Planetary Science,* 43, 139-166.

633 Francois, R., Honjo, S., Manganini, S.J., & Ravizza, G.E. (1995). Biogenic barium fluxes to the deep sea:
634 Implications for paleoproductivity reconstruction, *Global Biogeochemical Cycles*, 9, 289-303.
635 doi:10.1029/95GB00021.

636 Galloway, W.E., Ganey-Curry, P.E., Li, X., & Buffler, R.T. (2000), Cenozoic depositional history of the
637 Gulf of Mexico basin, *AAPG Bulletin*, 84, 1743-1774.

638 Gertsch, B., Keller, G., Adatte, T., Garg, R., Prasad, V., Berner, Z., & Fleitmann, D. Environmental effects
639 of Deccan volcanism across the Cretaceous–Tertiary transition in Meghalaya, India, *Earth and*
640 *Planetary Science Letters* **310** 272-285 (2011).

641 Gibbs, S.J., Bralower, T.J., Bown, P.R., Zachos, J.C., & Bybell, L.M. (2006). Shelf and open-ocean
642 calcareous phytoplankton assemblages across the Paleocene-Eocene Thermal Maximum:
643 Implications for global productivity gradients. *Geology*, 34, 233-236.

644 Gooday, A.J., (2003), Benthic Foraminifera (Protista) as tools in deep-water palaeoceanography:
645 environmental influences on faunal characteristics, *Advances in Marine Biology*, 46, 1–90.

646 Gradstein, F.M., Ogg, J.G., Schmitz, M., & Ogg, G., Eds. (2012), *The Geologic Times Scale 2012*.
647 Elsevier B.V., Amsterdam, Netherlands.

648 Griffith, E.M., & Paytan, A. (2012). Barite in the ocean–occurrence, geochemistry and
649 palaeoceanographic applications. *Sedimentology*, 59, 1817-1835.

650 Gulick, S.P., Barton, P.J., Christeson, G.L., Morgan, J.V., McDonald, M., Mendoza-Cervantes, K.,
651 Pearson, Z.F., Surendra, A., Urrutia-Fucugauchi, J., Vermeesch, P.M., & Warner, M.R. (2008).
652 Importance of pre-impact crustal structure for the asymmetry of the Chicxulub impact
653 crater. *Nature Geoscience*, 1, 131.

654 Gulick, S., Morgan, J., Mellett, C.L., Green, S.L., Bralower, T., Chenot, E., Christeson, G., Claeys, P.,
655 Cockell, C., Coolen, M.J.L., Ferrière, L., Gebhardt, C., Goto, K., Jones, H., Kring, D., Lofi, J.,
656 Lowery, C., Ocampo-Torres, R., Perez-Cruz, L., Pickersgill, A.E., Poelchau, M., Rae, A.,
657 Rasmussen, C., Rebolledo-Vieyra, M., Riller, U., Sato, H., Smit, J., Tikoo, S., Tomioka, N.,
658 Urrutia- Fucugauchi, J., Whalen, M., Wittmann, A., Yamaguchi, K., Xiao, L., & Zylberman, W.,

659 2017. Site M0077: Post-Impact Sedimentary Rocks. *In* Morgan, J., Gulick, S., Mellett, C.L.,
660 Green, S.L., and the Expedition 364 Scientists, *Chicxulub: Drilling the K-Pg Impact*
661 *Crater.* Proceedings of the International Ocean Discovery Program, 364: College Station, TX
662 (International Ocean Discovery Program). https://doi.org/10.14379/iodp.proc.364.105.2017

663 Gulick, S.P.S., Bralower, T.J., Ormö, J., Hall, B., Grice, K., Schaefer, B., Lyons, S., Freeman, K.H.,
664 Morgan, J.V., Artemieva, N., Kaskes, P., de Graff, S.J., Whalen, M.T., Collins, S.M., Verhagen,
665 C., Christeson, G.L., Claeys, P., Coolen, M.J., Goderis, S., Goto, K., Grieve, R., McCall, N.,
666 Osinksi, G.R., Rae, A., Riller, U., Smit, J., Vajda, V., Wittman, A., and Expedition 364 Scientists,
667 (*In Press*) The First Day of the Cenozoic. *Proceedings of the National Academy of Sciences*.

668 Hemleben, C., Spindler, M., & Anderson, O. R. (1989). *Modern planktonic foraminifera*. Springer
669 Science & Business Media.

670 Hemleben, C., Mühlen, D., Olsson, R.K., & Berggren, W.A. (1991). Surface texture and the first
671 occurrence of spines in planktonic foraminifera from the early Tertiary. *Geologisches Jahrbuch*,
672 128, 117-146.

673 Hildebrand, A.R., Penfield, G.T., Kring, D.A., Pilkington, M., Camargo, A.Z., Jacobsen, S.B., & Boynton,
674 W.V., 1991. Chicxulub Crater: a possible Cretaceous/Tertiary boundary impact crater on the
675 Yucatán Peninsula, Mexico. Geology 19, 867–871.

676 Hsü, K.J., & McKenzie, J.A. (1985). A "Strangelove" ocean in the earliest Tertiary. *The Carbon Cycle and*
677 *Atmospheric CO: Natural Variations Archean to Present*, 487-492.

678 Hull, P.M., & R.D. Norris (2011), Diverse patterns of ocean export productivity change across the
679 Cretaceous-Paleogene boundary: New insights from biogenic barium, Paleoceanography, 26(3).

680 Hull, P. M., Norris, R. D., Bralower, T. J., & Schueth, J. D. (2011). A role for chance in marine recovery
681 from the end-Cretaceous extinction. *Nature Geoscience*, 4, 856-860.

682 Jablonski, D. (1995) in *Extinction Rates* (eds. Lawton, J. H. & May, R. M.) 25–44 Oxford Univ. Press,
683 Oxford.

684 Jehle, S., Bornemann, A., Deprez, A., & Speijer, R.P. (2015). The impact of the latest Danian event on
685 planktic foraminiferal faunas at ODP site 1210 (Shatsky rise, Pacific Ocean). *PloS one*, 10,
686 e0141644.

687 Jiang, S., T.J. Bralower, M.E. Patzkowsky, L.R. Kump, &J.D. Schueth (2010), Geographic controls on
688 nannoplankton extinction across the Cretaceous/Palaeogene boundary, Nature Geoscience, 3(4),
689 280.

690 Jones, H., Lowery, C.M., and Bralower, T. (*Accepted*). Delayed calcareous nannoplankton boom-bust
691 successions in the earliest Paleocene Chicxulub Crater. *Geology*.
692 https://doi.org/10.1130/G46143.1

693 Jorissen, F.J., H.C. de Stigter, & J.G.V. Widmark, (1995), A conceptual model explaining benthic
694 foraminiferal microhabitats, *Marine Micropaleontology*, 26, 3–15.

695 Keller, G. (1989). Extended Cretaceous/Tertiary boundary extinctions and delayed population change in
696 planktonic foraminifera from Brazos River, Texas. *Paleoceanography and Paleoclimatology*, 4,
697 287-332.

698 Kominz, M.A., Browning, J.V., Miller, K.G., Sugarman, P.J., Mizintseva, S., & Scotese, C.R. (2008).
699 Late Cretaceous to Miocene sea-level estimates from the New Jersey and Delaware coastal plain
700 coreholes: an error analysis. *Basin Research*, 20, 211-226.

701 Knoll, A.H. & Follows, M.J. (2016) A bottom-up perspective on ecosystem change in Mesozoic oceans,
702 *Proceedings of the Royal Society B* 283 2016755.

703 Kring, D. A. (2007). The Chicxulub impact event and its environmental consequences at the Cretaceous–
704 Tertiary boundary: *Palaeogeography*, *Palaeoclimatology*, *Palaeoecology*, 255, 4-21.

Leckie, R.M., & H.C. Olson, (2003), Foraminifera as proxies for sea-level change on siliciclastic margins, *in*: Olson, H.C., and R.M. Leckie, eds., *Micropaleontologic proxies for sea-level change and stratigraphic discontinuities, SEPM Special Publication No. 75*, 5–19.

Lirer, F. (2000). A new technique for retrieving calcareous microfossils from lithified lime deposits. *Micropaleontology* 46, 365-369.

Liu, C., & Olsson, R.K. (1992). Evolutionary radiation of microperforate planktonic foraminifera following the K/T mass extinction event. *The Journal of Foraminiferal Research*, 22, 328-346.

Lowery, C.M. et al., 2018, Rapid Recovery of Life At Ground Zero of the End Cretaceous Mass Extinction, *Nature* v. 558, p. 288-291, https://doi.org/10.1038/s41586-018-0163-6

Lowery, C.M. & Fraass, A.J. (2019). Explanation for delayed recovery of species diversity following the end Cretaceous mass extinction. *Nature Ecology and Evolution* https://doi.org/10.1038/s41559-019-0835-0

Lowery, C.M., Bralower, T.J., Christeson, G., Gulick, S.P.S., Morgan, J.V., and Expedition 364 Scientists (2019). Ocean Drilling Perspectives on Meteorite Impacts. *Oceanography* 32, 120-134. https://doi.org/10.5670/oceanog.2019.133

MacLeod, K. G., Quinton, P. C., Sepúlveda, J., & Negra, M. H. (2018). Postimpact earliest Paleogene warming shown by fish debris oxygen isotopes (El Kef, Tunisia). *Science*, 360(6396), 1467-1469.

Morgan J.V. & 34 others, 2016, The formation of peak rings in large impact craters, *Science* 354, 878-882.

Morgan, J.V., S.P.S. Gulick, C.L. Mellet, S.L. Green, & Expedition 364 Scientists (2017) *Chicxulub: Drilling the K-Pg Impact Crater, Proceedings of the International Ocean Discovery Program, 364*, International Ocean Discovery Program, College Station, TX, doi: 10.14379/iodp.proc.364.103.2017.

727 Murray, J.W. (1976), A method of determining proximity of marginal seas to an ocean, *Marine Geology*,
728 22, 103–119.

729 Norris, R. D. (1996). Symbiosis as an evolutionary innovation in the radiation of Paleocene planktic
730 foraminifera. *Paleobiology*, 22, 461-480.

731 Okada, H., and Bukry, D. (1980). Supplementary modification and introduction of code numbers to the
732 low-latitude coccolith biostratigraphic zonation (Bukry, 1973; 1975). *Marine Micropaleontology*,
733 5, 321-325.

734 Olsson, R. K., Berggren, W. A., Hemleben, C. I., & Huber, B. T. (1999). Atlas of Paleocene planktonic
735 foraminifera. *Smithsonian Contributions to Paleobiology* 85.

736 Paytan, A., Kastner, M., and Chavez, F.P. (1996). Glacial to interglacial fluctuations in productivity in the
737 equatorial Pacific as indicated by marine barite. *Science*, 274, 1355-1357.

738 Paytan, A., and Griffith, E.M. (2007). Marine barite: Recorder of variations in ocean export productivity,
739 in *Encyclopedia of Paleoclimate and Ancient Environments*, Gornitz, V., Ed., p. 643-651, Springer,
740 New York.

741 Pearson, P.N., Olsson, R.K., Huber, B.T., Hemleben, C., and Berggren, W. A. (2006). Atlas of Eocene
742 Planktonic Foraminifera, Cushman Foundation for Foraminiferal Research Special Publications,
743 vol. 41. Washington, DC, 513.

744 Pedersen, T. F., & Calvert, S. E. (1990). Anoxia vs. productivity: what controls the formation of organic-
745 carbon-rich sediments and sedimentary Rocks?. *AAPG Bulletin*, *74*(4), 454-466.

746 Perch-Nielsen, K. (1985). Cenozoic calcareous nannofossils. *In* Bolli, H.M., Saunders, J.B., and Perch-
747 Nielsen, K. (Eds.) *Plankton stratigraphy*, Cambridge: Cambridge University Press. 427-554.

748 Punekar, J., Mateo, P., & Keller, G. (2014a) Effects of Deccan volcanism on paleoenvironment and planktic
749 foraminifera: A global survey, *Geological Society of America Special Papers,* 505, 91-116.

750 Punekar, J., Keller, G., Khozyem, H., Hamming, C., Adatte, T., Tantawy, A.A., & Spangenberg, J.E.
751 (2014b) Late Maastrichtian–early Danian high-stress environments and delayed recovery linked to
752 Deccan volcanism, *Cretaceous Research*, 49, 63-82.

753 Quillévéré, F., Norris, R.D., Kroon, D., and Wilson, P.A. (2008). Transient ocean warming and shifts in
754 carbon reservoirs during the early Danian. *Earth and Planetary Science Letters*, 265, 600-615.

755 Renne, P.R., Sprain, C.J., Richards, M.A., Self, S., Vanderkluysen, L., & Pande, K. (2015) State shift in
756 Deccan volcanism at the Cretaceous-Paleogene boundary, possibly induced by impact, *Science,*
757 350**,** 76-78.

758 Schoene, B., Eddy, M. P., Samperton, K. M., Keller, C. B., Keller, G., Adatte, T., & Khadri, S. F. (2019).
759 U-Pb constraints on pulsed eruption of the Deccan Traps across the end-Cretaceous mass
760 extinction. *Science*, *363*(6429), 862-866.

761 Schueth, J. D., T. J. Bralower, S. Jiang, and M. E. Patzkowsky (2015), The role of regional survivor
762 incumbency in the evolutionary recovery of calcareous nannoplankton from the
763 Cretaceous/Paleogene (K/Pg) mass extinction, Paleobiology, 41(4), 661-679.

764 Schulte, P. and 40 others, (2010), The Chicxulub asteroid impact and mass extinction at the Cretaceous-
765 Paleogene boundary, Science, 327, 1214-1218.

766 Smit, J. and J. Hertogen (1980). An extraterrestrial event at the Cretaceous-Tertiary boundary, Nature 285:
767 198-200.

768 Sprain, C. J., Renne, P. R., Vanderkluysen, L., Pande, K., Self, S., & Mittal, T. (2019). The eruptive tempo
769 of Deccan volcanism in relation to the Cretaceous-Paleogene boundary. *Science*, *363*(6429), 866-
770 870.

771 Thunell, R.C. (1976). Optimum indices of calcium carbonate dissolution, in deep-sea sediments. *Geology*,
772 4, 525-528.

773 Troelsen, J.C. (1957). Some planktonic foraminifera of the type Danian and their stratigraphic
774 importance. *US National Museum Bulletin*, 215, 125-131.

775 Van der Zwaan, G.J., Jorissen, F.J. & Stitger, H.C. (1990), The depth dependency of planktonic/benthic
776 foraminiferal ratios: constraints and applications, *Marine Geology*, 95, 1–16.

777 Van Hinsbergen, D.J.J., Kouwenhoven, T.J., & Van der Zwaan, G.J. (2005), Paleobathymetry in the
778 backstripping procedure: correction of oxygenation effects on depth estimates, *Palaeogeography,*
779 *Palaeoclimatology, Palaeoceology*, 21, 245–265.

780 Vellekoop, J., Sluijs, A., Smit, J., Schouten, S., Weijers, J.W.H., Sinninghe Damsté, J.S., & Brinkhuis, H.,
781 (2014). Rapid short-term cooling following the Chicxulub impact at the Cretaceous–Paleogene
782 boundary. *PNAS*, 111, 7537-7541.

783 Vellekoop, J., Woelders, L., Açikalin, S., Smit, J., Van De Schootbrugge, B., Yilmaz, I.O., Brinkhuis, H.,
784 & Speijer, R. (2017). Ecological response to collapse of the biological pump following the mass
785 extinction at the Cretaceous-Paleogene boundary. *Biogeosciences*, 14, 885-900.

786 Wade, B.S., Pearson, P.N., Berggren, W.A., & Pälike, H. (2011). Review and revision of Cenozoic tropical
787 planktonic foraminiferal biostratigraphy and calibration to the geomagnetic polarity and
788 astronomical time scale. *Earth-Science Reviews*, 104, 111-142.

789 Zachos, J.C., Arthur, M.A., & Dean, W.E. (1989). Geochemical evidence for suppression of pelagic marine
790 productivity at the Cretaceous/Tertiary boundary. *Nature*, 337, 61-64.

791